Doig, Barber. Published in AIAA Journal, 49(10), October 2011. 2330-2333

Considerations for Numerical Modeling of Inverted Wings in Ground Effect

Graham Doig* and Tracie J. Barber†
University of New South Wales, Sydney, New South Wales 2052, Australia

Nomenclature

b = span
C_D = drag coefficient
C_L = negative lift (downforce) coefficient
C_p = pressure coefficient
c = chord
h = height above the ground plane

Introduction

THE series of experiments conducted by Zerihan [1], Zerihan and Zhang [2,3], and Zhang and Zerihan [4–6] on an 80% scale model of the front wing of the 1998 Tyrell Formula One car (here referred to as the T-026 profile, based on a modified NASA GA(W) LS(1)-0413) have justifiably become the go-to source of validation for researchers investigating single and double element wings in ground effect (for example, [7–13]). This is due to the comprehensive nature of the tests, which included chordwise and spanwise pressure measurements for a large range of angles of attack and ground clearances (in terms of height-to-chord ratio, h/c), flow visualization, information about turbulent transition, offsurface measurements of wakes, vortices, and the general flowfield using both particle image velocimetry and laser doppler anemometry and force balance data for drag and downforce (negative lift).

Subsequent numerical investigations modeling this geometry have tended to focus on two-dimensional geometry representing the semispan point of the full wing ($z/b = 0$), and several studies have made comparisons between turbulence models and meshes in an attempt to determine the best approach for such flows [7–12]. While the original experiments for the wing detailed three-dimensional effects in considerable detail with regard to vortex behavior, spanwise pressure distributions, etc. [1], the wing had a fixed aspect ratio of 4.92 (corresponding to the real-world Formula 1 wing) and thus the true two-dimensionality of the wing at the semispan was not fully investigated. For this reason, some methodological issues associated with the interpretation of the data in two-dimensional comparisons have not been properly resolved, and to date it is not clear if a truly objective comparison of numerical schemes has been determined. While the influence of aspect ratio and wind-tunnel wall effects are well established for other oft-cited airfoils [14], lifting configurations rarely feature a finite wing with a short endplate at the tip and, thus the nature of the geometry in question here is largely unique to race car wings.

The two-dimensional computational results reported in literature indicate not only a persistent and significant overestimation of the suction peak of the lower surface, and thus an overprediction of lift coefficient [7–12], but also an unusually large spread of pressure distributions produced by different turbulence models [8]. Additionally, lift data has had to be compared with planar integrated pressure distributions instead of the force balance, and therefore there is no suitable drag data for comparison by this method, whereas the force balance provides this for the wing and endplate configuration. Other studies on other inverted wing geometries [15–17], comparing numerical results to wings of lower aspect ratios to the experimental results discussed here, may therefore suffer from the same misrepresentation of the measured flows.

The present investigation determines the applicability or otherwise of two-dimensional simulations of the T-026 wing and similar configurations, and in doing so characterizes any wall effects that may also be influencing experimental results obtained. To this end, five geometrically different models have been constructed for three different ground clearances, as noted in the case list in Table 1. These are a two-dimensional version with the tunnel roof represented, a two-dimensional version with no tunnel roof, a three-dimensional geometry complete with endplate, which includes the octagonal shape of the tunnel, one that ascribes a rectangular tunnel cross section, and one that features no side wall at all. The three-dimensional models feature a half-wing with a symmetry plane at the semispan ($z/b = 0$). Coordinates and dimensions of the wing and tunnel, respectively, can be found in the original documentation for the tests [1].

Numerical Method

The numerical method used to generate the present results has been extensively validated against the original experiments for a separate study into compressibility effects [13], and for the sake of brevity is merely outlined here. A commercial finite volume Reynolds-averaged Navier–Stokes solver, Fluent 6.3, was used to generate the results. The software is commonly used in the automotive industry. An implicit, pressure-based, coupled solver was applied to obtain steady-state solutions in 64-bit double precision. Grid independence of the three-dimensional structured hexahedral mesh (approx. 3.1×10^6 cells, y^+ of 1 on the wing) has previously been verified through extensive comparison to experiment [13], and in the present cases indicated a change of less than 0.05% in terms of pressure coefficient at any comparison point for two-dimensional runs with a directly quadrupled grid resolution.

The wing model was constructed to replicate the experiments as best as possible. Therefore, the endplates were included and meshed appropriately to capture the boundary layers there, and transition was imposed at $x/c = 0.1$. Transition in many cases in the experiments was found to result in a small separation over up to $0.03c$, potentially as a result of the type of grit strip used, and this feature is difficult to reproduce numerically and in the present case has not been accounted for. Transition on the endplate remains an unknown quantity. The freestream flow velocity was 30 ms^{-1}, giving a Reynolds number of approximately 4.6×10^5. The moving ground was represented (at a velocity matching the freestream, to ensure correct ground boundary representation [17]) from its foremost location, but ignores the leading edge of the elevated ground in which it rests, as this was not found to affect the ground flow to any great extent in the original tests. Turbulent intensity was set to 0.2% from the measured mean value. The wing was set at a "true" reference incidence as described in the

*Research Associate, School of Mechanical and Manufacturing Engineering, Kensington. Affiliate Member AIAA.
†Associate Professor, School of Mechanical and Manufacturing Engineering, Kensington.

Table 1 List of cases computed for T-026 wing

Case	2d/3d	h/c	Tunnel roof	Tunnel walls	Turb. model	C_L	C_D
Exp.				Freeflight			
1	2d	Freeflight	Y	n/a	Realizable k-ε	——	——
2	3d	Freeflight	Y	Square	Realizable k-ε	——	——
Exp.				0.313		1.04	0.040
3	2d	0.313	Y	n/a	Realizable k-ε	1.33	0.023
4	3d	0.313	Y	Square	Realizable k-ε	0.97	0.047
5	3d	0.313	Y	Square	SA	0.97	0.045
6	3d	0.313	Y	Square	SST	0.95	0.043
Exp.				0.179		1.28	0.055
7	2d	0.179	Y	——	Realizable k-ε	1.62	0.035
8	2d	0.179	N	——	Realizable k-ε	1.62	0.035
9	3d	0.179	Y	Square	Realizable k-ε	1.24	0.057
10	3d	0.179	Y	No	Realizable k-ε	1.24	0.056
11	3d	0.179	Y	Octagonal	Realizable k-ε	1.24	0.055
12	3d	0.179	Y	Square	SA	1.24	0.055
13	3d	0.179	Y	Square	SST	1.23	0.050
Exp.				0.067		1.38	0.076
14	2d	0.067	Y	Square	Realizable k-ε	1.41	0.066
15	3d	0.067	Y	Square	Realizable k-ε	1.39	0.077
16	3d	0.067	Y	Square	SA	1.39	0.076
17	3d	0.067	Y	Square	SST	1.35	0.072

literature as equating to 3.45° (anticlockwise, or nose-downward rotation from horizontal), with the ground clearance, defined in terms of h/c, measured from the chordwise point on the wing surface closest to the ground plane. An obvious omission from the model is the support struts, which held the wing in place in the tunnel. Unfortunately, little is known about the exact geometry of these struts but it is anticipated that their influence for the flow at the semispan is relatively small, less so for spanwise pressure measurements.

Three common turbulence models were used for a preliminary comparison; the one-equation Spalart–Allmaras (SA) model [18], the two-equation realizable k-ε model (used to produce the majority of results) [19], and the shear stress transport (SST) variant of the k-ω closure [20]. All of these models have previously been investigated in simulations of the airfoil section of this wing, with wide variations in effectiveness reported [7–9].

Results

The additional data in Table 1 highlighting predicted lift and drag coefficients indicates that the tunnel roof has a negligible effect, and the side wall whether in square configuration (simplified) or octagonal (real-world) has only a slight influence on the predicted drag (comparing cases 9, 10, and 11 at $h/c = 0.179$). This is possibly due in part to a very mild effect on the downstream path of the lower wing/endplate vortex which, particularly in the case of the octagonal section, may be affected by the relative proximity of the foot of the angled wall section. Its inclusion serves to correct the drag closer to the experimental value, but does not result in any appreciable difference in the predicted pressure distributions at the semispan, and therefore could be simplified to the square section unless vortex behavior was of particular interest in simulations.

The blockage is therefore low enough not to influence any results, and allows for a relatively concise computational domain. The walls could be modeled as slip surfaces without any great penalty to accuracy. The inclusion of the endplate, however, emerges as an important factor in determining the pressure distribution of the wing at the semispan. Comparisons have been made in Figs. 1–4 showing the predicted distribution at this location in comparison to experiments for different ground clearances [freestream ($h/c = 3.36$), $h/c = 0.313$, 0.179 and 0.067] at the reference incidence.

Even without any appreciable ground influence in Fig. 1, the difference between two-dimensional and three-dimensional cases is clear, with the three-dimensional case providing a much closer match to the experimental readings on the upper surface where the two-dimensional case overpredicts C_P over the forward half of the wing. On the lower surface it appears that the three-dimensional simulation better captures the extent of the suction peak, with the two-dimensional case again overpredicting here, though the two results slowly converge in the pressure recovery region to the trailing edge. Upstream of the suction peak, the two-dimensional case exhibits a much more pronounced suction spike close to the leading edge. As this is observed at $h/c = 0.313$ and 0.179, it is likely to be another facet of the two-dimensional case being unable to relax the flow in the spanwise direction.

Figure 2 indicates that the two-dimensional simulation at $h/c = 0.313$, with the ground now an influential factor, has corrected over the upper surface to offer a good comparison to experimental data, while still outperformed by the three-dimensional simulations with regard to the region at approximately $x/c = 0.05$ where the pressure plateau settles. On the suction surface, the two-dimensional simulation greatly exaggerates the suction peak at $x/c = 0.18$, and generally predicts more negative pressure over the whole lower surface, consistent with the results of Zerihan and Zhang [7] and Mahon and Zhang [8,9]. All three turbulence models tested in the three-dimensional case provide a better match to the experimental results, slightly underpredicting the suction peak. It is important to note that all three models produce virtually identical performance, in stark contrast to previously reported two-dimensional results [8].

This feature is repeated at the lower clearance of $h/c = 0.179$ in Fig. 3, where all three turbulence models again produce a highly similar pressure distribution, with mild variations at the suction peak within the approximate margin of error of the original experiments.

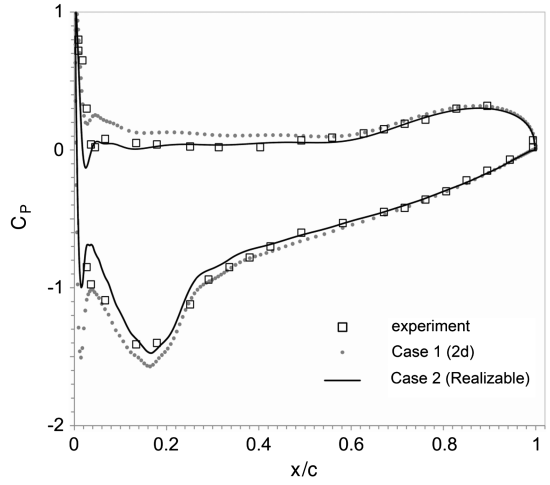

Fig. 1 Pressure coefficient distribution at the semispan for the wing in "freeflight" (no ground).

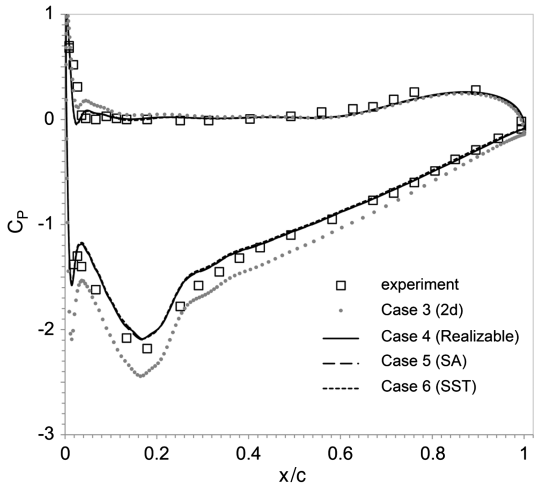

Fig. 2 Pressure coefficient distribution at the semispan for the wing at $h/c = 0.313$.

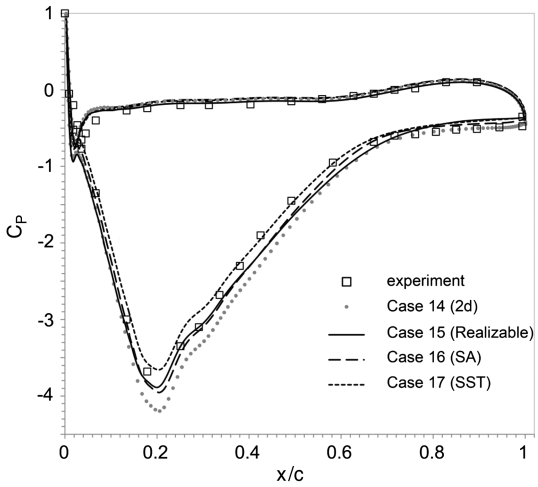

Fig. 4 Pressure coefficient distribution at the semispan for the wing at $h/c = 0.067$.

The two-dimensional simulation exaggerates the lower surface distribution by a greater margin than at the higher clearance, though the upper surface increasingly resembles the three-dimensional cases and the experimental results at all points.

These trends are repeated at $h/c = 0.067$, in Fig. 4, where the overshoot of peak suction from the two-dimensional case is greatest of all. There is notable discrepancy in the turbulence models at this clearance, which is the most complex investigated in that it features significant separation close to the trailing edge (itself variable across the span) and an effective "bursting" of the lower wing/endplate vortex [1,2,6]. While all compare favorably to the experimental measurements relative to the two-dimensional case, the k-ω SST model underpredicts the extent of the suction peak while the SA and realizable models perform less effectively in the pressure recovery region over the midchord to the trailing edge. It is difficult to determine the most effective model from this comparison alone, and further correlation with wake and vortex data would be required to make an informed decision.

The results imply that any numerical optimization of a two-dimensional profile for downforce, drag minimization, separation point, and natural transition control will not necessarily translate well when applied to a full three-dimensional wing with endplate, and even less so to a wing without an endplate, as the spanwise flow effect will be greater. The lift coefficient from a two-dimensional simulation is unlikely to compare well with an integration of the semispan pressure distribution unless that distribution is from an experiment featuring a high aspect ratio wing that spans a tunnel test section. Given the great advances in computing power and ease of mesh construction since the original experiments and some of the subsequent numerical simulations, it is clear that three-dimensional simulations should be performed when simulating racing car wings of aspect ratios of less than at least five.

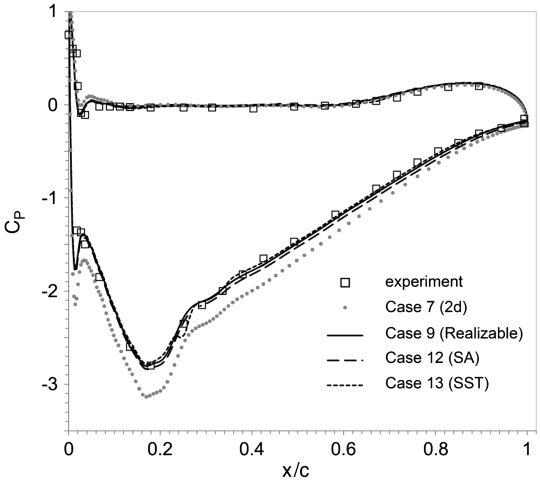

Fig. 3 Pressure coefficient distribution at the semispan for the wing at $h/c = 0.179$.

Conclusions

When conducting numerical modeling of an inverted racecar wing (of aspect ratio five or less) that has been wind-tunnel tested, it is unlikely that a two-dimensional simulation of the semispan will provide adequate comparison to experimental results, and instead overestimate the effectiveness of the profile. This has been demonstrated in the case of the T-026 wing for which a wealth of experimental data exists. It was found that the tunnel side walls and roof had only a small effect on drag, likely due to an influence on the lower surface wing/endplate vortex downstream, and can therefore be simplified or ignored in numerical modeling, which is only concerned with pressure distributions on the wing itself.

While the flow is effectively two-dimensional at the semispan, it exists at an equilibrium significantly influenced by the spanwise distortion to the flowfield from the endplates. The influence is actually lessened over the upper surface by a reduction ground clearance as the acceleration of flow around the wing has a normalizing effect, which reduces the extent of spanwise flow there; however, the same effect exaggerates the discrepancies for the lower surface. Three-dimensional simulations provided a much improved match to the experimental semispan pressure data in all cases, and highlighted close agreement between results from three common turbulence closures at all clearances bar $h/c = 0.067$, where more significant discrepancies emerged.

References

[1] Zerihan, J., "An Investigation into the Aerodynamics of Wings in Ground Effect," Ph.D. Thesis, Univ. of Southampton, School of Engineering Sciences, UK, 2001.

[2] Zerihan, J., and Zhang, X., "Aerodynamics of a Single Element Wing in Ground Effect," *Journal of Aircraft*, Vol. 37, No. 6, 2000, pp. 1058–1064.
doi:10.2514/2.2711

[3] Zerihan, J., and Zhang, X., "Aerodynamics of Gurney Flaps on a Wing in Ground Effect," *AIAA Journal*, Vol. 39, No. 5, 2001, pp. 772–780.
doi:10.2514/2.1396

[4] Zhang, X., and Zerihan, J., "Aerodynamics of a Double Element Wing in Ground Effect," AIAA Paper 2002-0834, 2002.

[5] Zhang, X., and Zerihan, J., "Off-Surface Aerodynamic Measurements of a Wing in Ground Effect," *Journal of Aircraft*, Vol. 40, No. 4, 2003, pp. 716–725.
doi:10.2514/2.3150

[6] Zhang, X., and Zerihan, J., "Edge Vortices of a Double Element Wing in

Ground Effect," *Journal of Aircraft*, Vol. 41, No. 5, 2004, pp. 1127–1137.
doi:10.2514/1.1380

[7] Zhang, X., and Zerihan, J., "A Single Element Wing in Ground Effect: Comparisons of Experiments and Computation," AIAA Paper 2001-423, Jan. 2001.

[8] Mahon, S., and Zhang, X., "Computational Analysis of Pressure and Wake Characteristics on an Aerofoil in Ground Effect," *Journal of Fluids Engineering*, Vol. 127, No. 2, 2005, pp. 290–298.
doi:10.1115/1.1891152

[9] Mahon, S., and Zhang, X., "Computational Analysis of an Inverted Double-Element Aerofoil in Ground Effect," *Journal of Fluids Engineering*, Vol. 128, No. 6, 2006, pp. 1172–1180.
doi:10.1115/1.2353268

[10] Wordley, S., and Saunders, J., "Aerodynamics for Formula SAE: A Numerical, Wind Tunnel and On-Track Study," SAE Paper 2006-01-0808, 2006.

[11] Doig, G., Barber, T. J., Leonardi, E., and Neely, A. J., "The Onset of Compressibility Effects for an Inverted Aerofoil in Ground Effect," *The Aeronautical Journal*, Vol. 111, No. 1126, 2007, pp. 797–806.

[12] Vogt, J. W., and Barber, T. J., "Variation of Ground Effect Phenomena About Downforce Generating Tyrrell and NACA4412 Aerofoils," *International Journal of Aerodynamics*, Vol. 1, No. 1, 2010, pp. 82–96.
doi:10.1504/IJAD.2010.031704

[13] Doig, G., Barber, T. J., and Neely, A. J., "The Influence of Compressibility on the Aerodynamics of an Inverted Wing in Ground Effect," *Journal of Fluids Engineering*, Vol. 33, No. 6, 2011, pp. 1–12.
doi:10.1115/1.4004084

[14] Garbaruk, A., Shur, M., Strelets, M., and Spalart, P. R., "Numerical Study of Wind-Tunnel Wall Effects on Transonic Airfoil Flow," *AIAA Journal*, Vol. 41, No. 6, 2003, pp. 1046–1054.
doi:10.2514/2.2071

[15] Ranzenbach, R., "Cambered Airfoil in Ground Effect: Wind Tunnel and Road Conditions," *Proceedings of the 13th AIAA Applied Aerodynamics Conference*, AIAA, Reston VA, 1995, pp. 1208–1215.

[16] Ranzenbach, R., and Barlow, J., "Two Dimensional Aerofoil in Ground Effect, Experimental and Computational Study," *SAE International Congress & Exposition*, SAE Paper 942509, 1994.

[17] Barber, T. J., Leonardi, E., and Archer, R. D., "Causes for Discrepancies in Ground Effect Analyses," *The Aeronautical Journal*, Vol. 106, No. 1066, 2002, pp. 653–667.

[18] Spalart, P., and Allmaras, S., "A One-Equation Turbulence Model for Aerodynamic Flows," AIAA Paper 92-0439, 1992.

[19] Shih, T. H., Liou, W. W., Shabbir, A., Yang, Z., and Zhu, J., "A New k-ε Eddy-Viscosity Model for High Reynolds Number Turbulent Flows: Model Development and Validation," *Computers and Fluids*, Vol. 24, No. 3, 1995, pp. 227–238.
doi:10.1016/0045-7930(94)00032-T

[20] Menter, F. R., "Two-Equation Eddy-Viscosity Turbulence Models for Engineering Applications," *AIAA Journal*, Vol. 32, No. 8, 1994, pp. 1598–1605.
doi:10.2514/3.12149